APPLIED HYDROCARBON THERMODYNAMICS

VOLUME 2

SECOND EDITION
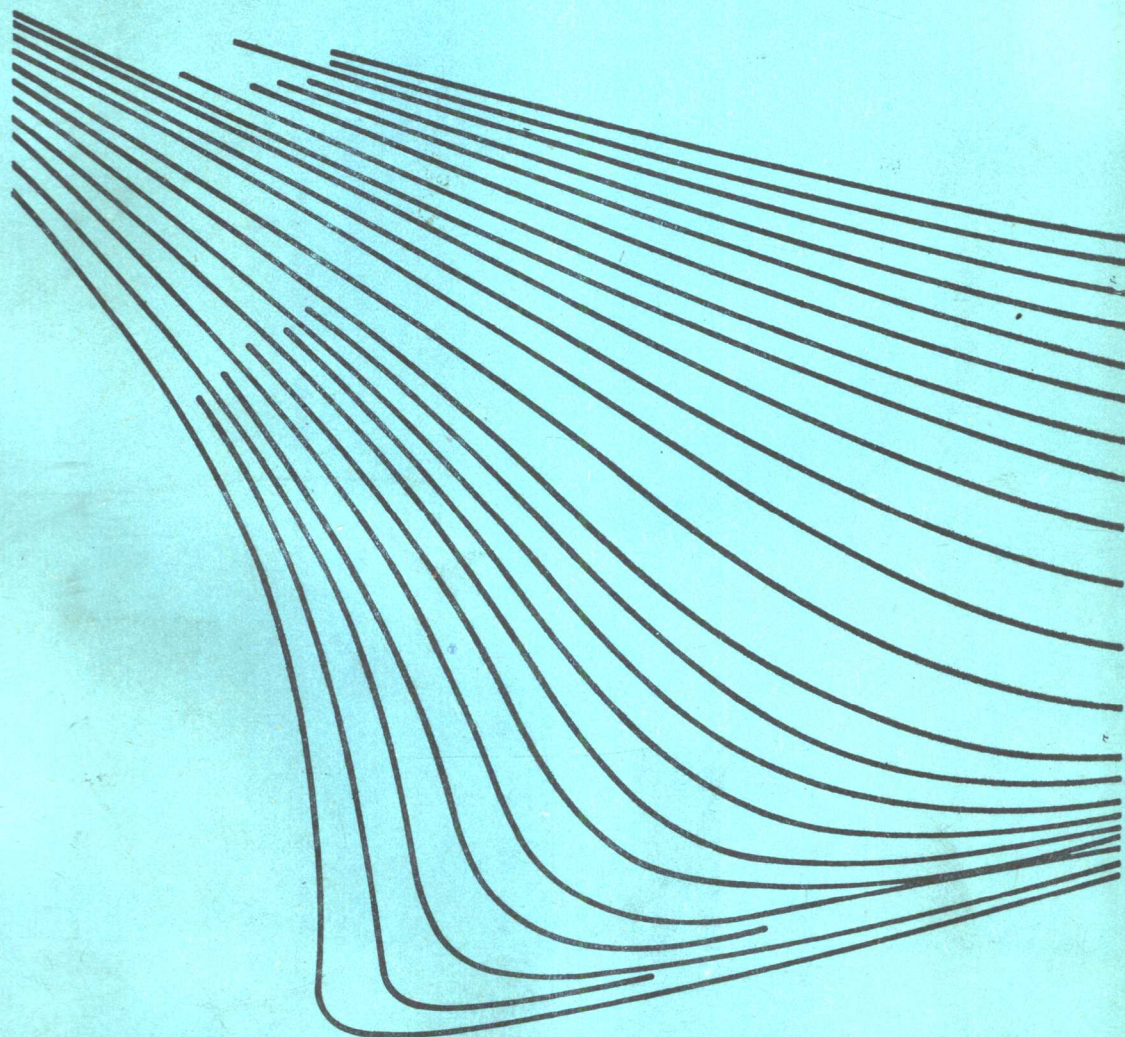
WAYNE C. EDMISTER

APPLIED
HYDROCARBON
THERMODYNAMICS
VOLUME 2
SECOND EDITION

WAYNE C. EDMISTER
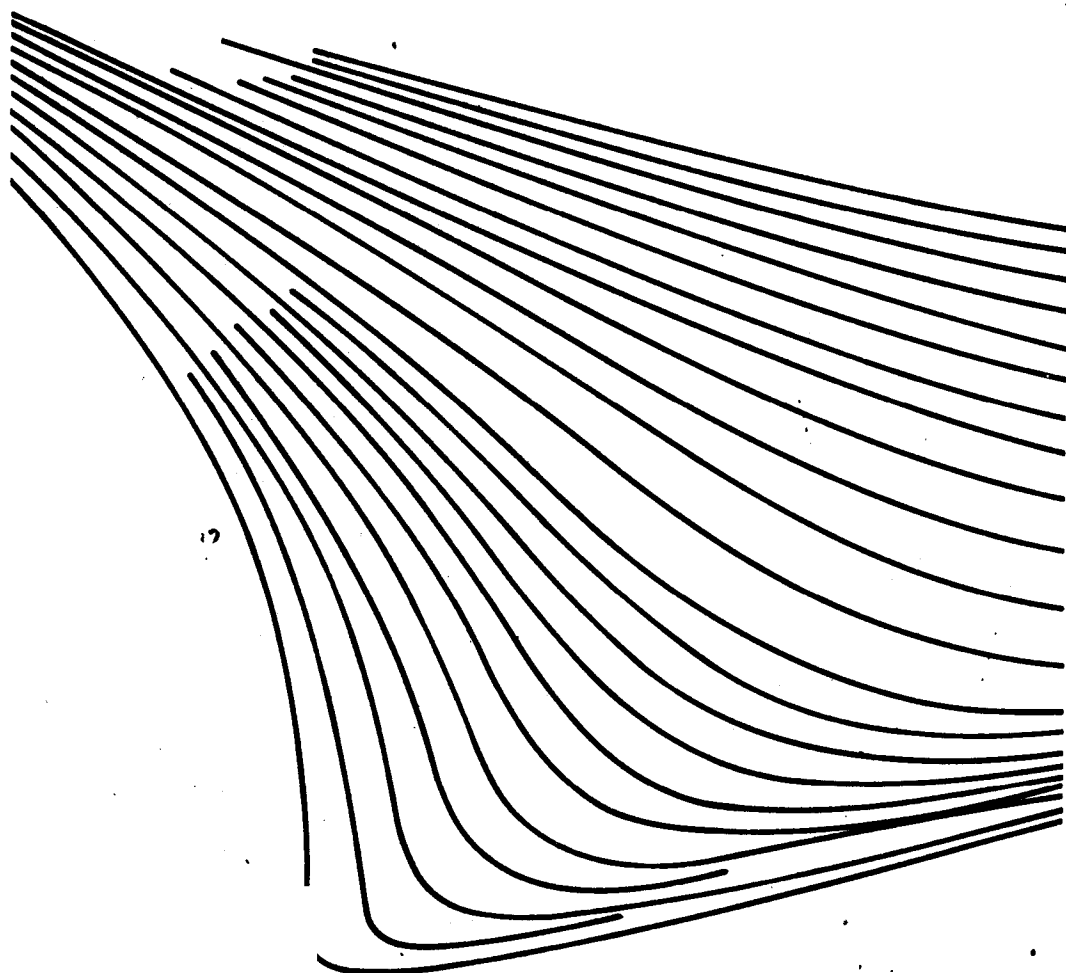
Applied Hydrocarbon Thermodynamics

VOLUME 2, SECOND EDITION

Acknowledgments

Foreword

This volume completes the second edition of Professor Edmister's *Applied Hydrocarbon Thermodynamics*. The objective of the second edition has been the same as for the first edition; namely to provide a source of practical information and tools for process engineers to use in thermodynamic property prediction, simulation, and design calculations.

Although the overall objective of the second edition is the same as that of the first edition, the information and tools are now different. Process engineers use computer hardware and software more than they use charts and slide rules in their work today. With this in mind the author has developed computer programs and data banks for vapor liquid equilibria, reaction equilibria, and other process calculations, all based upon the same basic theory, as presented in Volume 1 of this second edition.

Of special interest to petroleum refining process engineers will be Professor Edmister's pseudo component technique and computer method for characterizing petroleum fractions in phase equilibrium calculations, in which discrete and pseudo components get the fugacity-type K-value treatments.

Another unique part of this work includes material on the thermochemical properties of petroleum fractions in Chapters 24 and 25, where a modified method of corresponding states was applied to calculate the heats of combustion, formation, and reaction, and free energy of formation for petroleum fractions.

This volume will prove valuable to engineering students and practitioners in chemical and petroleum process development and design.

John J. McKetta
Chairman
Editorial Committee
Hydrocarbon Processing
Houston, Texas

Preface

Volume 1 of this second edition of *Applied Hydrocarbon Thermodynamics* contains ten chapters of fundamentals, properties data, and charts. The theoretical concepts and mathematical derivations included in Volume 1 prepare the way for the development of the ultimate thermodynamic tool—computer programs for applying thermodynamics to hydrocarbon process simulation and design. Such programs are the objective of this second edition of Volume 2.

Programs were first prepared and tested on a mainframe computer and then downloaded to a personal computer for further development. The capacity, speed, and convenience of the micro, or PC, computer have increased greatly during the past few years, making it ideal hardware for applications of thermodynamics. FORTRAN programs for this were written in a user-interactive format. Complete source codes are not included, but an executable version of the programs is available separately. The software development work is described in this volume, with examples of the subprograms, input data, and results.

Special features of interest are a data bank for 213 hydrocarbons and associated gases; computer breakdown of petroleum fractions into 11 or 21 pseudo components from ASTM or TBP assays of the oil; acceptance of narrow petroleum cuts as hypothetical components in the feed; bubble and dew point temperature or pressure calculations; alternate flash calculations to find unknown temperature, pressure, or vapor fraction; enthalpy or entropy balance flashes; adiabatic/polytropic compression and expansion design calculations for gases; compressible fluid flow calculations; enthalpies at alternate datum states; heats of chemical reactions and chemical reaction equilibria; and thermochemical properties and absolute enthalpies of petroleum fractions.

To capsulize this volume: Chapter 11 introduces the reader to thermodynamic properties and process simulation; Chapters 12 and 13 contain the graphical phase equilibria correlations for petroleum fractions from the previous edition; Chapters 14 and 15 repeat the intégral technique and pseudo-components of petroleum fractions from the previous edition, with additional examples; Chapters 16 and 17 give background information on computer predictions and then describe the subroutines of the computer algorithm; Chapter 18 defines the three alternate zero enthalpy datum states, gives a computer program for calculating constants for converting to each datum, and gives the conversion constants for all 213 hydrocarbons in Block Data; Chapters 19 and 20 present gas compression and calculation methods and compressible fluid flow through orifices and pipes. Included are some first edition material and new computer programs. Chapters 21 and 22 cover heats of reaction and reaction equilibrium, with some first edition material repeated and a new computer program presented; Chapter 23 covers the construction of *H-X* diagrams with information repeated from the first edition, plus new items; Chapters 24 and 25 present all new material on enthalpies of combustion and formation and free energies of formation, plus alternate zero enthalpy states for petroleum fractions.

Wayne C. Edmister
San Rafael, California

Contents

11

Introduction—Thermodynamic Properties and Process Simulation

Scope of this Book

Volume 1 of this two-volume set presented the basic thermodynamic tools (charts, tables, and equations) needed to make phase and energy calculations in hydrocarbon process design. It included theoretical concepts and mathematical derivations, and thus prepared the way for this volume's development of the ultimate thermodynamic tool—a computer program for actually applying thermodynamics to hydrocarbon processing.

Hardware and Software

The thermodynamic properties and vapor-liquid equilibrium programs described in this second volume of *Applied Hydrocarbon Thermodynamics* are in FORTRAN 77 for mainframe and microcomputers (IBM compatible).

The FORTRAN source code files were first prepared, compiled, linked, and tested on the mainframe. Then the source code files were down-loaded to the micro, where they were again compiled, linked, and run. This micro-computer work was done with the MicroSoft FORTRAN compiler.

Complete FORTRAN source code versions of the programs are not included in this book, but compiled and linked versions are available in executable form. I have tried to describe the programs clearly enough to allow the reader to prepare his or her program if desired.

Basis of Discussion

Some of the important basic topics related to vapor-liquid equilibrium calculations (designated VLE throughout this text for convenience) were covered in Volume 1's Chapters 3, 9, and 10. For example, the criteria for phase equilibria were discussed in Chapter 3, while the definition and usage of the VLE K-values were presented in Chapter 9, including several methods for making vapor-liquid equilibrium calculations. In Chapter 10, the K-value relationships with other properties, such as the vapor pressure and fugacity, were reviewed and some graphical K-value correlations were presented.

The manual calculation methods discussed in Chapters 9 and 10 were primarily intended for background information on VLE calculations and K-values. Even with the over-simplified assumptions normally used, the manual methods are very tedious, time consuming, and of limited accuracy, particularly for multicomponent mixtures. Accordingly, such manual methods are seldom used in engineering practice now, being replaced by the more accurate rigorous methods.

This volume discusses computer methods for making K-value predictions and VLE calculations for hydrocarbon mixtures and petroleum fractions, with or without

associated gases. Special emphasis is given to a newly developed VLE program, named EQUIL.

Program Requirements

A workable program for making VLE and thermodynamic properties calculations for complex mixtures needs

1. A data bank for the discrete components of interest.
2. Methods for converting petroleum fractions into pseudo-components and predicting their characterizing properties.
3. Methods for making equilibrium calculations for single and multiple stage processes.
4. Methods of converging the iterative calculation inherent in the calculations.
5. A program for creating input data files and an output file handling and printing system.
6. A user-interactive system to permit operating the program conveniently from a keyboard.

Component Properties

Properties of hydrocarbons were tabulated in Chapter 7 of Volume 1. These data have been put into a data file for convenient reading by the program. This file, identified as BLOCK DATA, is an integral part of EQUIL, the computer program. Similar properties for the pseudo components of petroleum fractions must be found by empirical equations. The technique for breaking petroleum fractions into pseudo components and finding the necessary property values are given in Chapters 14 and 15 of this volume, following graphical equilibrium flash vaporization correlations for petroleum in Chapters 12 and 13.

Solution Methods

Methods of converging to unknown temperatures, pressures, vapor/liquid fractions, enthalpies, and/or entropies are covered in Chapter 16, as are the eleven possible phase equilibria processes with specified and unknown variables. Chapter 16 also presents the six source code files containing more than 50 subprograms that make up the master program that has been the objective of this work. Descriptions of these subprograms are presented in Chapter 17. Chapter 18 covers alternate zero enthalpy datum states for pure components, Chapter 25 for petroleum components.

Other topics covered in this volume include flow of compressible fluids in Chapter 19; gas compression and expansion calculations in Chapter 20; heats of chemical reactions in Chapter 21; chemical reaction equilibria in

Chapter 22; enthalpy-composition diagrams in Chapter 23; thermochemical properties of petroleum fractions in Chapter 24; and absolute enthalpies of petroleum fractions in Chapter 25.

The rest of this chapter describes several phenomena of vapor liquid equilibria and reviews basic fugacity relationships, thus establishing the basis for the preparation of the actual programs.

Multicomponent Phase Equilibria

This section reviews the phase behavior of multicomponent mixtures and describes retrograde condensation/vaporization phenomena, different VLE processes (bubble and dew points, isothermal or constant temperature and pressure flash, constant pressure and vapor fraction flash, constant temperature and vapor fraction flash, isenthalpic flash, and isentropic flash), and methods of solving the complex mathematical expressions.

An understanding of the nature and types of phase equilibria, commonly encountered in hydrocarbon processing calculations, is important to having a working knowledge of the calculation procedures. Hydrocarbon mixture separations into the many constituents, such as pure components, gasoline, naphtha, kerosene, diesel oil, gas oil, fuel oil etc., by vaporization, condensation, and distillation are the hydrocarbon processes of interest here.

As distillation consists of a series of equilibrium stages, accurate K-values and VLE calculations are critical in designing hydrocarbon separation processes, as was illustrated in Volume 1's Chapter 9. In such process design work, it is sometimes necessary to predict three-phase equilibria for vapor-liquid-liquid (VLLE), in addition to VLE, for hydrocarbon mixtures containing non-hydrocarbons, such as water, carbon dioxide, and/or hydrogen sulfide.

Another phase equilibrium state frequently encountered in hydrocarbon processing is that of hydrates forming at low temperatures from water and some hydrocarbons, and/or CO_2 and H_2. Though less frequent, there are other types of phase equilibrium encountered in hydrocarbon processing—vapor-solid, liquid-liquid, vapor-liquid-solid, vapor-solid-solid, liquid-solid-solid, vapor-liquid-liquid-solid, and vapor-liquid-solid-solid. This chapter deals only with vapor-liquid phase equilibrium.

Vapor-Liquid Equilibria

Figure 11.1 is a typical pressure-temperature diagram for a mixture of fixed composition, in which the curves B and D represent the bubble-point and dew-point loci,
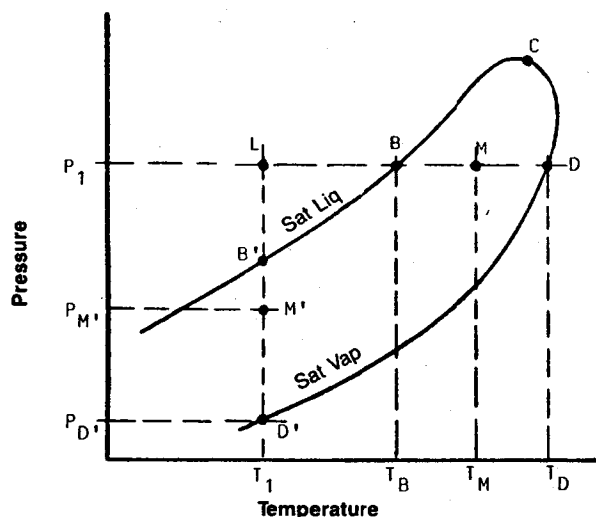
Figure 11.1. A typical *P-T* diagram for a mixture of given composition.

respectively, and point *C* is the critical point of the mixture. The envelope formed by the bubble-point and dew-point curves is commonly called the "phase boundary" or "saturated" phase envelope. Liquid that exists along the bubble-point curve *B* is "saturated liquid" because the liquid cannot retain any more molecules in the liquid state when there is an infinitesimal change in the pressure or temperature toward the inner area of the phase envelope. Similarly, the vapor along the dew-point curve *D* is "saturated vapor."

On the other hand, liquid outside the bubble-point curve is "subcooled liquid" and vapor outside the dew-point curve is "superheated vapor." For example, the point *L* (at P_1 and T_1) represents a subcooled liquid. This liquid becomes saturated at point *B*, if the temperature is increased to T_B at constant P_1. At this point, the first tiny bubble of vapor is about to appear in the liquid, yet the composition of the liquid remains unchanged.

However, if the temperature is increased further, the liquid starts to vaporize, forming a vapor with a different composition from that of the liquid. Consequently, the liquid composition also changes as the vaporization proceeds with the increase in temperature. For example, at point *M* (P_1 and T_M), inside the phase envelope, both vapor and liquid phases coexist and their compositions are different, not only from each other but also from the original liquid *L*. As the temperature increases, the amount of vapor also increases until the last tiny drop of liquid is about to disappear at T_D. At this point, the composition of the vapor (saturated) becomes identical to that of the original liquid *L*, and the composition of the last drop of liquid is completely different from the original liquid. If the temperature is increased further, the va-

por becomes "superheated," and the composition remains unchanged. Similar phenomena occur when the pressure varies along $L\,B'\,M'\,D'\,V''$ at constant temperature T_1.

The purpose of VLE calculations is to determine the conditions and the phase compositions at such points as *B, M, D, B', M',* or *D'*. The phase equilibrium calculations along the bubble-point curve (*B* or *B'*) and along the dew-point curve (*D* or *D'*) are commonly called *bubble-point calculations* and *dew-point calculations*, respectively. Those VLE calculations made at conditions inside the two-phase envelope are called *flash calculations*.

Bubble Points and Dew Points

It should be obvious that there are two types of bubble-point calculations for a mixture—one is to find the bubble-point temperature and the composition of the coexisting equilibrium vapor at a given pressure, e.g., point *B* in Figure 11.1; the other calculation is to find the bubble-point pressure and the composition of the coexisting equilibrium vapor at a given temperature, e.g., point *B'*. Similarly, the point *D* represents the dew-point temperature calculation at P_1, and point *D'* represents the dew-point pressure calculation at T_1.

From a mathematical point of view, the bubble- or dew-point calculation is made to determine $(n + 1)$ unknowns from the following $(n + 1)$ equations for a mixture of *n* components:

$$\bar{f}^L_i(T,P,\bar{X}) = \bar{f}^V_i(T,P,\bar{Y}), \quad i = 1,2,...N \qquad (11.1)$$

$$\sum_1^N y_i = 1.0 \text{ for bubble point}$$

$$\left(\text{or } \sum_1^N x_i = 1.0 \text{ for dew point}\right) \qquad (11.2)$$

where T = temperature
P = pressure
$\bar{X}$ = liquid mole fraction, vector
$\bar{Y}$ = vapor mole fraction, vector

The fugacity identity, Equation 11.1, was discussed in Chapters 3 and 10, whereas Equation 11.2 was given in Chapter 9 as Equation 9.42 or 9.43. For bubble-point temperature calculations, the $n + 1$ unknowns are the temperature T and the vapor composition $y_i(i = 1,2,...N)$. Similarly, for dew-point pressure calculations, the $(n + 1)$ unknowns are the pressure and the liquid composition, i.e., the P and x_i values.

Equilibrium Flash Vaporizations

Perhaps the most familiar flash is the so-called isothermal flash, which is also isobaric, as represented by M and M' in Figure 11.1. The isothermal flash calculation is made to find the vapor fraction (V/F) and the vapor and liquid compositions. The relationships of the vapor and liquid compositions are illustrated by the pressure-temperature diagram in Figure 11.2 for a two-component mixture. In this diagram, Comp 1 and Comp 2 represent the pure component vapor pressures for components 1 and 2, respectively, and the three-phase envelopes I, II, and III represent three different compositions of the two component mixtures. Each envelope is similar to that in Figure 11.1.
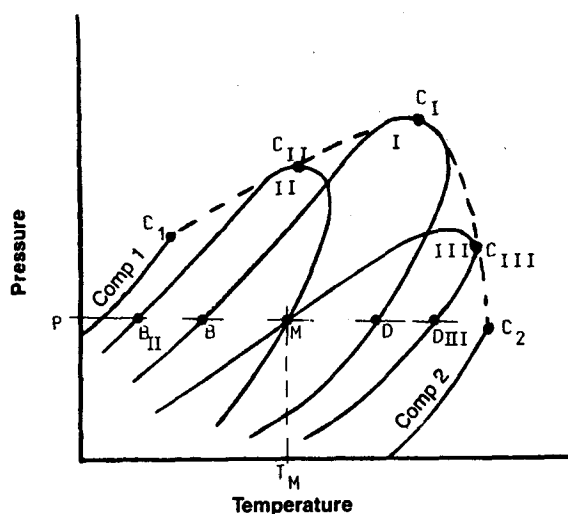
Figure 11.2. A typical diagram for several compositions of a binary system.

When the mixture I is brought to the condition given by M (at P and T) its vapor phase composition is the same as that of mixture II, and its liquid phase composition is the same as that of mixture III. Although Figure 11.2 is for a two-component mixture, the same relationship also holds for multicomponent mixtures.

Mathematically, the isothermal flash calculation is made to find ($2n + 1$) unknowns from a set of ($2n + 1$) equations for an n-component mixture. These ($2n + 1$) unknowns are the vapor fraction (V/F), and the $y_i (i = 1,2,..N)$ and $x_i (i = 1,2,..N)$ values. The ($2n + 1$) equations include Equations 11.1 and 11.2, and the following n material balance equations that were discussed in Chapter 9.

$$z_i = (V/F)y_i + (1 - V/F)x_i, \quad i = 1,2,...N \tag{11.3}$$

where F = total moles of given feed mixture
V = total moles of equilibrium vapor
z_i = feed mole fraction

It should be obvious from Equations 11.1 through 11.3 that the equations may also be solved for T, y_i, and x_i from the known values of P, V/F, and z_i. This type of flash calculation is often called "constant vapor-fraction flash" or "constant liquid-fraction flash."

As discussed earlier, the vapor fraction (V/F) is uniquely determined at each temperature between B and D at constant pressure between B and D at constant pressure P_1 in Figure 11.1, with its value varying from 0 at point B to 1 at point D. Indeed the constant vapor fraction flash calculation at constant P is identical to the bubble-point temperature calculation when $V/F = 0$, and is identical to the dew-point temperature calculation when $V/F = 1$. It should be noted that Equation 11.3 becomes $z_i = x_i$ when $V/F = 0$, which is the bubble-point requirement, and also reduces to $z_i = y_i$ when $V/F = 0$, which is a required condition for the dew point.

Retrograde Phenomenon

The one-to-one relationship of V/F to the temperature at constant pressure does not always hold true. Figure 11.3 illustrates an example of a phase condition with two temperatures for a given V/F at constant pressures. Note first that there are two bubble points, B_1 and B_2, at a given pressure P_B between the critical pressure P_C and the maximum pressure P_{MAX}. If the temperature is increased from point B_1 at constant P_B, the vapor fraction (V/F) gradually increases from $V/F = 0$ at B_1 to the max-

Figure 11.3. Mixture P-T diagram showing boundary curve points in critical region.

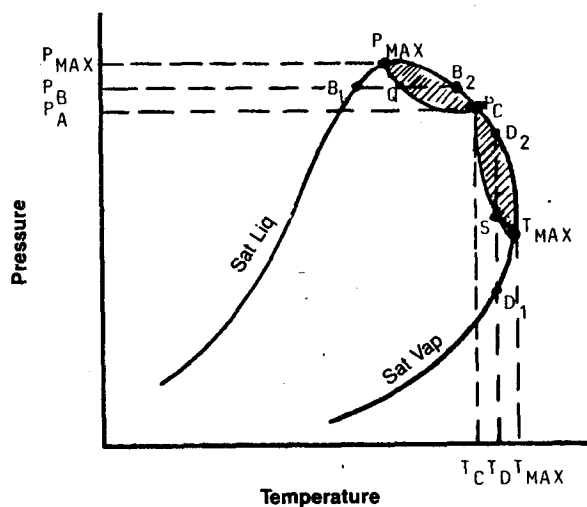imum value of V/F (smaller than unity) at point Q, then decreases with a further increase in temperature, finally becoming $V/F = 0$ again at B_2, i.e., to completely condensed.

This phenomenon, appropriately called *retrograde condensation*, occurs at all pressures in the shaded area between P_C and P_{MAX}. Because of the occurrence of retrograde condensation, there are two identical values of V/F corresponding to two different temperatures at constant pressure; one between B_1 and Q, and the other between Q and B_2. In other words, there exist two sets of valid solutions for T, y_i, and x_i for a given value of V/F and P between P_C and P_{MAX}. Therefore, once a solution is obtained in this region, it is important to identify the location of the solution by making another flash calculation (either isothermal flash at P_B and $T = T + \Delta T$, or constant vapor fraction flash at P_B and $V/F = V/F + \Delta(V/F)$) in the vicinity of the original solution to check whether or not V/F increases with the increase in temperature. If it does, the solution is clearly between B_1 and Q; if it does not, the solution may be assumed to be between Q and B_2. It is obvious that the specified value of V/F must not exceed the maximum value in making flash calculations in the retrograde region.

A phenomenon called *retrograde vaporization*, similar to the retrograde condensation, also occurs in the shaded area between T_C and T_{MAX} on the dew-point curve side of the phase diagram, Figure 11.3. For instance, if the pressure is increased from D_1 at constant T_D, the amount of liquid also increases from D_1 at $L = 0$ to the maximum value at S, then decreases with a further increase in pressure, finally becoming $L = 0$ again at D_2, i.e., to completely vaporize at D_2. This retrograde vaporization occurs at all temperatures in the shaded area between T_C and T_{MAX}. Like in the case of retrograde condensation, there are two sets of valid solutions for T, y_i, and x_i with a given V/F value and with T between T_C and T_{MAX}; one between D_1 and S, and the other between S and D_2. In this case, a procedure similar to the one just described for retrograde condensation may be followed to find the location of the desired solution.

This retrograde condensation (or vaporization) region, which is also loosely called the critical region, is a difficult area for VLE calculations, i.e., the solution often fails to converge, or converges to a trivial solution for which $y_i = x_i$ for all components, primarily resulting from the numerical sensitivity of the calculations to the variables (T, y_i, x_i, or P, y_i, x_i) and also from the poor accuracy of the thermodynamic models used in the computation methods.

As shown in the shaded area of Figure 11.4, the retrograde condensation (or vaporization) region is located just below the critical locus, which is the locus of the critical points, connected by a dashed line on Figure 11.2. This locus can be easily obtained for a two-compo-
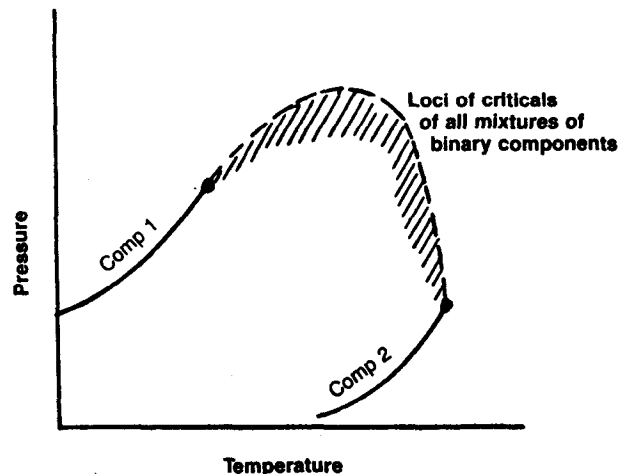
Figure 11.4. Mixture P-T boundary curve showing retrograde condensation and vaporization regions.

nent mixture by drawing a series of phase envelopes between the two vapor pressure curves of the two pure components and then connecting their critical points. Such critical loci are also shown as "convergence pressure curves" in Figure 10.13 and Figures 10.18 through 10.25. The region bounded by the two pure component vapor pressure curves and the critical locus, as shown in Figures 11.2 and 11.4, is called the "two-phase region" for this system.

The relative locations of critical points on the liquid-vapor phase boundary curves are shown in Figure 11.5, which is from Rowlinson (15). Critical points shown are C, the true critical point; CT, the cricondentherm point; and CB, the cricondenbar point. The names "cricondentherm" and "cricondenbar" were first proposed in 1934 by Sage et al. (16) to define the points of maximum temperature and maximum pressure on the phase boundary diagram.

Three mixture types in this illustration are I, normal proportions of light and heavy components; II, lighter component dominating; and III, heavier component dominating. The dashed lines through the critical point are the loci of other mixtures of the same components. From these diagrams, it can be seen that the true critical point, C, is located in between CB and CT for mixture Type I, whereas C is located on the BP side for Type II and on the DP side for Type III.

Useful Features of the Mixture Phase Diagram

Vapor/liquid phase boundary diagrams, such as those shown on Figures 11.1 through 11.5, are formed by the joining of two curves at the critical point. These are the

Type (I) Mixture
Normal Proportions
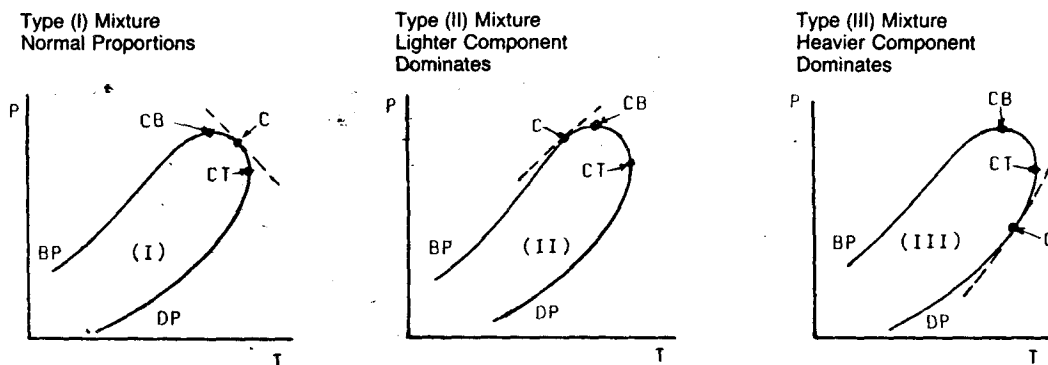
Type (II) Mixture
Lighter Component
Dominates

Type (III) Mixture
Heavier Component
Dominates

Figure 11.5. Relative locations of critical points for mixtures. (Dashed lines are loci of critical points: C—critical point; CT—cricondentherm point; CB—cricondenbar point.) (From Rowlinson, 1959.)

bubble point (0% vapor) and the dew point (100% vapor) curves, sometimes called "boundary curves." The area within these boundary curves is the "co-existing equilibrium vapor and liquid" region, i.e., the temperature-pressure combinations at which vapor and liquid will co-exist in equilibrium.

If lines of constant fraction vaporized are drawn within such a phase diagram, the result would be a family of curves that converge at the critical point at their upper ends and fan out in a gradual, uniform and conforming way at their lower ends. Boundary diagrams containing such lines of constant percent vapor are sometimes called P-T-X diagrams.

The boundary curves for the three mixture types shown on Figure 11.5 could be made into P-T-X diagrams by adding these percent vaporized lines. The top portions of these curves would contain some reversals.

Figure 11.6 contains P-T plots for ethane and n.-heptane and for three mixtures of these two hydrocarbons, i.e., the vapor pressure curves for ethane and n-heptane plus the boundary curves for the three mixtures. These plots were made from experimental data obtained by Kay (14). The dashed curved line is the critical locus, drawn through the five critical points. The dashed straight line is the pseudo critical locus for this system, which was defined by Kay as the molar average of the critical temperatures and pressures of the mixture components.

Boundary curves, of the type shown in Figure 11.6, can be obtained accurately for binary mixtures of known composition by an experimental procedure that requires measuring only temperatures and pressures. These temperature and pressure readings are plotted to obtain boundary curves for several compositions.

From these charts, pressure versus composition cross-plots are made. Figure 11.7 shows pressure-composition cross-plots for five isotherms of the methane-ethane system, from Price and Kobayaski (22). From these P-X

plots, it is a simple matter to calculate $K = y/x$ values. This K-value method (experimental measurements plus graphical calculations) is limited to binary systems.

To illustrate the use of charts like Figure 11.7, find the K-values for methane and ethane at $-50°F$ and 700 psia. Read from Figure 11.7: m.f.s C_2 in vapor = 0.18; in liquid = 0.464. Complete calculations as follows:

	Ethane	Methane
Vapor	0.180	$1.0 - 0.180 = 0.82$
Liquid	0.464	$1.0 - 0.464 = 0.536$
$K = y/x$	$0.180/0.464 = 0.388$	$0.820/0.536 = 1.530$

This method can be used for binaries only.

Binary Interaction Coefficients

In Volume 1's Chapter 5, Equations 5.68 and 5.69 include the term k_{ij}, binary interaction coefficient, in combining the equation of state constants for components to obtain the values for mixtures by both Soave-RK and Peng-Robinson EOS's. The use of such binary interaction coefficients with equations of state is one of the reasons for the superiority of the Soave-RK (28) and the Peng-Robinson (21) EOS methods over the Chao-Seader and the Lee-Erbar-Edmister methods, which used an EOS for the vapor phase only and used empirical equations for the liquid phase properties.

Values of k_{ij} for use in VLE predictions are derived from P-T-X-Y measurements on a binary system by iterative calculations made to find a single k_{ij} value that gives the best agreement for calculated pressure, or another mixture property, with the experimental value for the same binary system. The experimental data used must be thermodynamically consistent and the derivation calculations must be made with the same EOS that the k_{ij} values are to be used with.
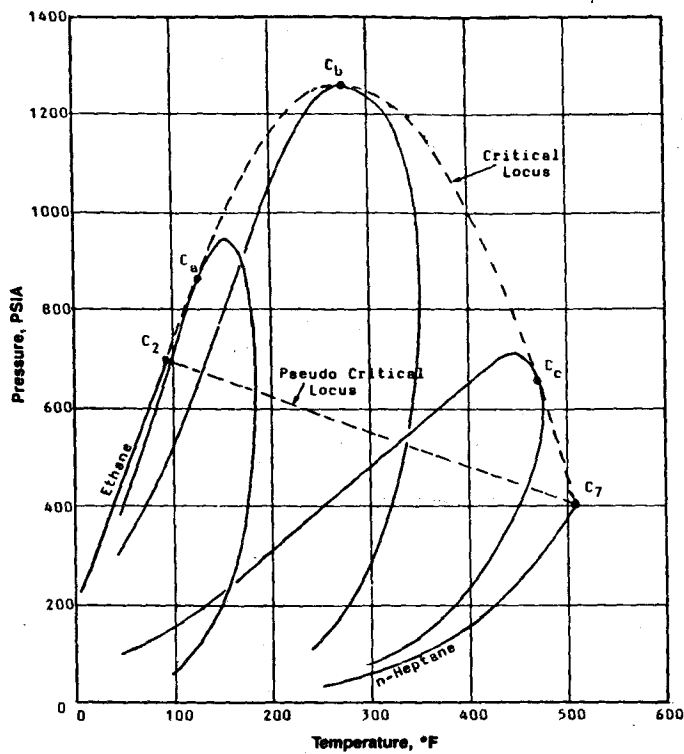
Figure 11.6. Critical loci for ethane, n-heptane, and three binaries. Wt. % C_2H_6: $C_2 = 100.0$; $C_a = 90.22$; $C_b = 50.25$; $C_7 = 0.0$. (From Kay, 1938.)
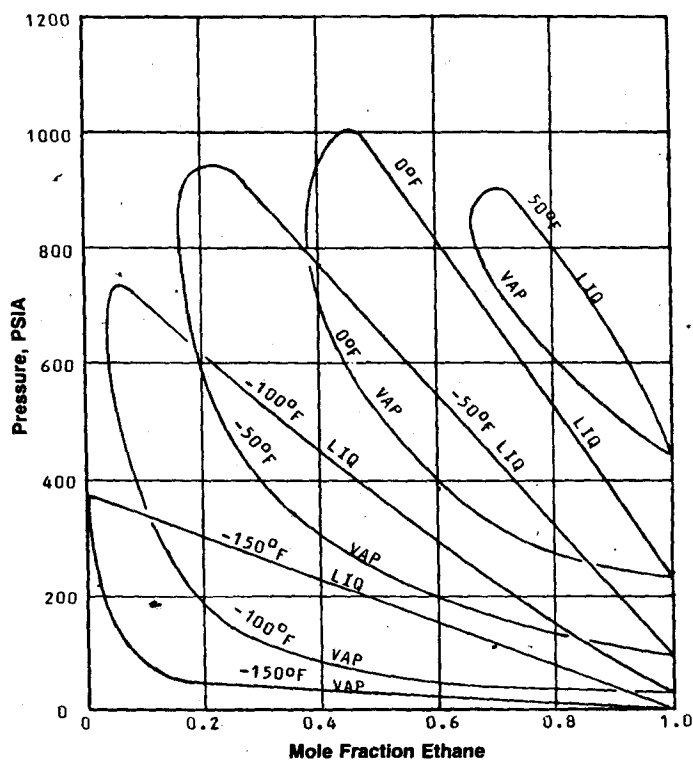

Figure 11.7. Pressure composition diagram for methane-ethane system. (From Price and Kobayaski, 1959.)

Ideally the optimum value of k_{ij} should minimize the errors in the prediction of all thermodynamic properties calculated from the EOS. In practice, one property like bubble-point pressure is used. The techniques for finding these binary interaction coefficients are described by Daubert et al. (6, 9), who defined and used an objective function of pressure, Q.

$$Q = \sum_{1}^{N} ((p_c - p_e)/p_e)^2 \qquad (11.4)$$

where N = number of points
c = calculated pressure
e = experimental pressure.

Paunovic et al. (20) proposed and used a fugacity objective function, as follows:

$$Q = \sum_{1}^{N} [\{(FV1 - FL1)/FV1\}^2$$

$$+ \{(FV2 - FL2)/FV2\}^2] \qquad (11.5)$$

where N = number of points
$FV1$ = fugacity of component 1 in vapor
$FL1$ = fugacity of component 1 in liquid
$FV2$ = fugactiy of component 2 in vapor
$FL2$ = fugacity of component 2 in liquid

With either of these functions, the procedure is to calculate Q for assumed values of k_{ij}, then plot Q against k_{ij}, and find the optimum k_{ij} at the minimum Q point on that plot. In evaluating Q by Equation 11.4, it is necessary to converge an equilibrium pressure calculation. Finding Q by Equation 11.5 is simpler in that no convergence is necessary; the fugacities are evaluated at the conditions of the experimental data.

For hydrocarbon systems containing non-hydrocarbons, such as CO_2, H_2S, CO, and N_2, the use of k_{ij} values is necessary. For hydrocarbons of the same kind, i.e., paraffin binaries or olefin binaries, k_{ij} values are not usually required. Consult References 12, 18, 19, 21, and 28 at the end of this chapter for more information.

The optimum value of k_{ij} will now be found for the carbon dioxide-normal hexane system, using the experimental data of Kalra et al. (12) and the Soave (28) EOS. P-T-X-Y data were complete and had been checked for thermodynamic consistency by the authors. An abridged tabulation, showing one-third of these data, is given in Table 11.1. It can be seen that the data are at temperatures from 99.5 to 399.3°F and pressures up to 1,931 psia.

Table 11.1
Experimental P-T-X-Y Data for Carbon Dioxide -nHeptane for Deriving Binary Interaction Coefficients (12)

Temperature °F	Pressure psia	Mol Fractions CO_2 Liquid	Vapor
99.5	30.5	0.0250	0.9490
	128.0	0.1000	0.9840
	526.0	0.4140	0.9930
	948.0	0.8350	0.9930
	1097.0	0.9490	0.9500
175.0	61.5	0.0310	0.8600
	230.0	0.1260	0.9560
	960.0	0.4980	0.9740
	1426.0	0.7150	0.9630
	1684.0	0.8478	0.9050
250.0	164.0	0.0730	0.8190
	450.0	0.1930	0.9210
	906.0	0.3760	0.9420
	1505.0	0.5890	0.9340
	1931.0	0.7680	0.8820
399.3	254.0	0.0420	0.3440
	720.0	0.2190	0.6810
	1228.0	0.4160	0.7680
	1439.0	0.5550	0.6380

Values of Q were computed at 24 evenly spaced values of k_{ij} ranging from 0.0 to 0.24, using Equation 11.5 and the Soave-RK EOS, and the resulting Q values were plotted against k_{ij} in Figure 11.8. Note that the curve through these points has a minimum Q value at $k_{ij} = 0.114$. This is the binary interaction coefficient for these data and the Soave-RK EOS.

Isenthalpic and Isentropic Processes

The preceding discussions were limited to flash processes in the two-phase region, wherein the variables considered were temperature, pressure, the fraction vaporized, and compositions of vapor and liquid. Other processes of interest are isenthalpic (constant enthalpy) and isentropic (constant entropy) processes, which are not restricted to either single- or two-phase conditions. Both isenthalpic and isentropic processes can occur without a phase change, i.e., the initial and/or final condition may be in the superheated vapor or the subcooled liquid states.

The isenthalpic process is sometimes called an adiabatic flash, even though the process may occur in the vapor or liquid single-phase region. Isenthalpic and isentropic processes are not really flashes in the true sense.